

A robust synchronization method for grid sequence extraction

Abstract. A robust synchronization method based on least mean square is proposed for the real time detection of fundamental and harmonic symmetrical components, including positive, negative and zero sequence. The new architecture is composed of three parallel structures providing estimation of each phase fundamental and harmonic components delivered into a linear matrix transformation for grid sequence extraction. To achieve frequency adaptation, a combination of least mean square and phase locked loop is used. The paper presents excellent simulation and experimental results in order to verify correctness and validity of the algorithm.

Streszczenie. W artykule opisano opracowaną metodę synchronizacji z siecią, wykrywającą w czasie rzeczywistym częstotliwość podstawową oraz wyższe harmoniczne, w tym składową zgodną, przeciwną i zerową. Architektura składa się z trzech równoległych estymatorów harmonicznych dla każdej fazy. Po przetworzeniu danych i wyznaczeniu składowych, dokonywana jest synchronizacja, z wykorzystaniem metody najmniejszych kwadratów oraz PLL. Przedstawione zostały wyniki symulacyjne i eksperymentalne. (Algorytm synchronizacji częstotliwościowej w ekstrakcji składowych symetrycznych w sieci).

Keywords: Grid connected converters, least mean square, phase locked loop, symmetrical components

Słowa kluczowe: przekształtniki sieciowe, metoda najmniejszych kwadratów, PLL, składowe symetryczne

Introduction

Synchronization with the utility network is a crucial point for controlling grid connected converters, especially under unbalanced and distorted conditions [1, 2]. Among the many applications of synchronization algorithms are flexible AC transmission systems (FACTS) [3-5], series or shunt active filters [6, 7], distributed power generation systems [8-12], and uninterruptible power supplies [13]. Additionally, The precise detection of fundamental and harmonic symmetrical components is essential for power flux calculations, or selective harmonic compensation [14, 15]. Therefore, the robust synchronization method for grid sequence extraction is expected.

In general, for three phase applications, an ideal synchronization method should: 1) provide the phase and frequency information of the utility signal. 2) track the fundamental and harmonic grid sequence components variation. 3) work well under distorted utility conditions, such as harmonics, line notching, voltage unbalance, etc. 4) be implemented with the low computational burden.

Various synchronization algorithms have been proposed in recent years. The simplest strategy of obtaining the phase information is zero crossing method whose dynamic performance is influenced by harmonics and white noise [16-18]. Synchronous reference frame phase locked loop (SRF-PLL) is widely used in three phase systems [19, 20]. Under ideal conditions without distortion or unbalance in utility networks, SRF-PLL with a high bandwidth yields a fast and precise detection of the phase and amplitude of the utility voltage vector. SRF-PLL can also operate correctly if only high order harmonics are present in the grid voltages, by reducing its bandwidth to attenuate these harmonics. However, under unbalanced conditions, the second harmonic content of the voltage vector, caused by the negative sequence components, makes the reduction of the bandwidth an inefficient solution, since the dynamics response speed of the PLL would become very slow for such a narrow bandwidth.

In order to solve the abovementioned problem, several improved schemes based on modified PLL have been proposed. For instance, the decoupled double synchronous reference frame PLL (DDSRF-PLL) [21] overcomes the unbalance drawback by using a decoupling cell to isolate the positive and negative sequence components. Although the advanced synchronization system is capable of making an accurate estimation of the fundamental components of the voltage under unbalanced conditions, the performance of the scheme may be severely affected by harmonics

present in the three phase signals.

Dual second order generalized integrator PLL (DSOGI-PLL) [22-24] is another typical approach. It utilizes quadrature signals generator to extract the fundamental positive sequence. However, these detected signals may be affected by low order harmonics and subharmonics. Furthermore, the SOGI needs the grid frequency estimation for its correct operation. This frequency can be obtained from the output of SRF-PLL. Nevertheless, due to the complexity of the resulting nonlinear closed loop scheme, it is difficult to design the parameters in order to ensure stability or some desired transient performance.

A technique using the enhanced PLL (EPLL) [25] for each phase is presented in [26], named as 3ph-EPLL. The phase voltages and their 90 degrees phase shift version reconstructed by the EPLL are used for obtaining the fundamental positive sequence voltages, utilizing the instantaneous symmetrical components (ISC) method. Finally, another EPLL is applied to the output of the ISC method to estimate the phase angle of positive sequence voltages. Although the fundamental negative sequence components of the grid voltages are eliminated by the EPLL calculator, some harmonics will pass through the EPLL and may be present in its output.

This paper proposes a grid synchronization scheme aimed to provide an estimation of fundamental and harmonic grid sequence components present in three phase voltages. It is demonstrated that the new strategy consists of three similar adaptive notch filters based on the concept of least mean square (LMS) algorithm, a symmetrical components calculator and a PLL based phase angle estimator. In fact, the technique without coordinate transformation can be widely used for three phase three wire and three phase four wire systems.

Proposed Strategy

1 Signal Tracking Based on LMS

In power system, a three phase set of unbalanced and distorted signals can be represented as

$$(1) \quad \begin{cases} u_a = \sum_{n=1}^N U_a^n \sin(n\omega_k T_s + \phi_a^n) \\ u_b = \sum_{n=1}^N U_b^n \sin(n\omega_k T_s + \phi_b^n) \\ u_c = \sum_{n=1}^N U_c^n \sin(n\omega_k T_s + \phi_c^n) \end{cases}$$

where U_i^n and ϕ_i^n are the magnitude and initial phase angle of n th harmonic component in phase i ($i = a, b, c$), ω is the fundamental frequency, T_s is the sampling interval and k is the sampling instant. The phase angle of fundamental component in phase a is described by:

$$(2) \quad \omega k T_s + \phi_a^1 = \theta_a + \varphi_a$$

where θ_a is the estimated value of $\omega k T_s + \phi_a^1$, and φ_a is the estimated error. Therefore, the phase angle of n th harmonic component in phase i is obtained:

$$(3) \quad \begin{cases} n\omega k T_s + \phi_a^n = n\theta_a + n\varphi_a + \phi_a^n - n\phi_a^1 \\ n\omega k T_s + \phi_b^n = n\theta_a + n\varphi_a + \phi_b^n - n\phi_a^1 \\ n\omega k T_s + \phi_c^n = n\theta_a + n\varphi_a + \phi_c^n - n\phi_a^1 \end{cases}$$

substituting (3) into (1), then the phase voltages can be rewritten as:

$$(4) \quad \begin{cases} u_a = \sum_{n=1}^N U_a^n \cos(n\varphi_a + \phi_a^n - n\phi_a^1) \sin(n\theta_a) \\ \quad + \sum_{n=1}^N U_a^n \sin(n\varphi_a + \phi_a^n - n\phi_a^1) \cos(n\theta_a) \\ u_b = \sum_{n=1}^N U_b^n \cos(n\varphi_a + \phi_b^n - n\phi_a^1) \sin(n\theta_a) \\ \quad + \sum_{n=1}^N U_b^n \sin(n\varphi_a + \phi_b^n - n\phi_a^1) \cos(n\theta_a) \\ u_c = \sum_{n=1}^N U_c^n \cos(n\varphi_a + \phi_c^n - n\phi_a^1) \sin(n\theta_a) \\ \quad + \sum_{n=1}^N U_c^n \sin(n\varphi_a + \phi_c^n - n\phi_a^1) \cos(n\theta_a) \end{cases}$$

To simplify analysis, only the fundamental frequency component is considered. Then, the above equation becomes as follows:

$$(5) \quad \begin{cases} u_a = U_a^1 \cos(\varphi_a) \sin(\theta_a) + U_a^1 \sin(\varphi_a) \cos(\theta_a) \\ u_b = U_b^1 \cos(\varphi_b) \sin(\theta_a) + U_b^1 \sin(\varphi_b) \cos(\theta_a) \\ u_c = U_c^1 \cos(\varphi_c) \sin(\theta_a) + U_c^1 \sin(\varphi_c) \cos(\theta_a) \end{cases}$$

where $\varphi_b = \varphi_a + \phi_b^1 - \phi_a^1$ and $\varphi_c = \varphi_a + \phi_c^1 - \phi_a^1$. Next, the model of equation (5) is utilized in the estimation of three phase fundamental components. Equation (5) suggests that the original signal can be reconstructed by adjusting the weight coefficients $U_i^1 \cos(\varphi_i)$, $U_i^1 \sin(\varphi_i)$ ($i = a, b, c$), even though the phase angle of phase a is unknown. Followed by this concept, adaptive linear filter with least mean square (LMS) rule is implemented to adjust the weight coefficients.

Firstly, the estimated signal can be expressed as:

$$(6) \quad \tilde{Y} = WX$$

where \tilde{Y} , W , X corresponding to the estimated output of the fundamental grid voltage, the weight vector, the input vector respectively, are represented as:

$$(7) \quad \tilde{Y} = [\tilde{u}_a \quad \tilde{u}_b \quad \tilde{u}_c]^T$$

$$(8) \quad W = \begin{bmatrix} W_{11} & W_{12} \\ W_{21} & W_{22} \\ W_{31} & W_{32} \end{bmatrix}$$

$$(9) \quad X = [X_1 \quad X_2]^T = [\sin(\theta_a) \quad \cos(\theta_a)]^T$$

The basic architecture of LMS is designated as an adaptive filter where the weight vector is adjusted in a recursive fashion toward its optimum value. In terms of the mathematical formulae, the weight vector is updated as [27, 28]:

$$(10) \quad W(k+1) = W(k) + \mu \frac{e(k)X(k)^T}{X(k)^T X(k)}$$

where $e(k)$ represents the estimated error expressed as follows:

$$(11) \quad \begin{aligned} e(k) &= [e_a \quad e_b \quad e_c]^T \\ &= [u_a - \tilde{u}_a \quad u_b - \tilde{u}_b \quad u_c - \tilde{u}_c]^T \end{aligned}$$

The step size μ in equation (10) is critical for controlling the convergence time as well as the level of misadjustment. When μ is small, the LMS algorithm takes more time to learn about its input with minimum mean square error and vice versa [29]. From (5), it can be deduced that if the following equation is satisfied:

$$(12) \quad W = \begin{bmatrix} U_a^1 \cos(\varphi_a) & U_a^1 \sin(\varphi_a) \\ U_b^1 \cos(\varphi_b) & U_b^1 \sin(\varphi_b) \\ U_c^1 \cos(\varphi_c) & U_c^1 \sin(\varphi_c) \end{bmatrix}$$

then, the desired signal will equal to its estimate. Hence, the three phase voltages can be regenerated by adjusting weight vector with LMS rule.

In addition, it is worth to remark that the orthogonal version of \tilde{Y} , i.e., 90 degrees phase shift version of \tilde{Y} , can also be obtained at the same time from another linear combination between input data vector and weight vector. The equation describing the quadrature signal is given by:

$$(13) \quad \tilde{Y}^\perp = W'X$$

where \tilde{Y}^\perp and W' corresponding to the orthogonal version of \tilde{Y} and the revised weight vector of W respectively, are represented as:

$$(14) \quad \tilde{Y}^\perp = [\tilde{u}_a^\perp \quad \tilde{u}_b^\perp \quad \tilde{u}_c^\perp]^T$$

$$(15) \quad W' = \begin{bmatrix} W_{11} & -W_{12} \\ W_{21} & -W_{22} \\ W_{31} & -W_{32} \end{bmatrix}$$

The scheme describing the estimation process of phase a is shown in Fig. 1. Summarizing, the proposed algorithm consists of three main blocks: 1) Least mean square (LMS) block can provide updated law of the weight vector. 2) Estimated signal generator (ESG) block can provide estimation of the input signal. 3) Quadrature signal generator (QSG) block can provide estimation of its 90 degrees phase shift version. The similar analysis can also be applied for phase b and c , hence it is omitted here. In steady state, φ_a can be considered to be zero. For the sake of brevity, assume that $\phi_a^1 = 0$. Therefore, (2) is rewritten to be $\omega k T_s = \theta_a$. Referring to fundamental component in phase a , the estimated value in discrete domain can be derived as:

$$\begin{aligned}
\tilde{u}_a &= W_{11} \sin(\omega k T_s) + W_{12} \cos(\omega k T_s) \\
(16) \quad &= \left(\sum_{j=0}^{k-1} \mu e_a(j) \sin(\omega j T_s) \right) \sin(\omega k T_s) \\
&\quad + \left(\sum_{j=0}^{k-1} \mu e_a(j) \cos(\omega j T_s) \right) \cos(\omega k T_s)
\end{aligned}$$

Applying z transform to (16), the transfer function is given by:

$$(17) \quad G'(z) = \frac{\tilde{u}_a(z)}{e_a(z)} = \frac{\mu(1 - z^{-1} \cos \omega T_s)}{T_s(1 - 2z^{-1} \cos \omega T_s + z^{-2})}$$

where $\tilde{u}_a(z)$ and $e_a(z)$ correspond to the z transform of \tilde{u}_a and e_a , respectively. Fig. 2 shows the discrete bode plot of $G'(z)$ where $T_s = 0.2ms$ is assumed. It can be observed that it exhibits as a typical notch filter at the fundamental frequency point. The effect of step size μ in the frequency response is that higher step size results in higher attenuation. From the plot, it can be concluded that frequency characteristic of LMS is similar to SOGI in attenuating harmonics. Furthermore, the proposed algorithm can extract harmonics with modified structure which will be discussed later.

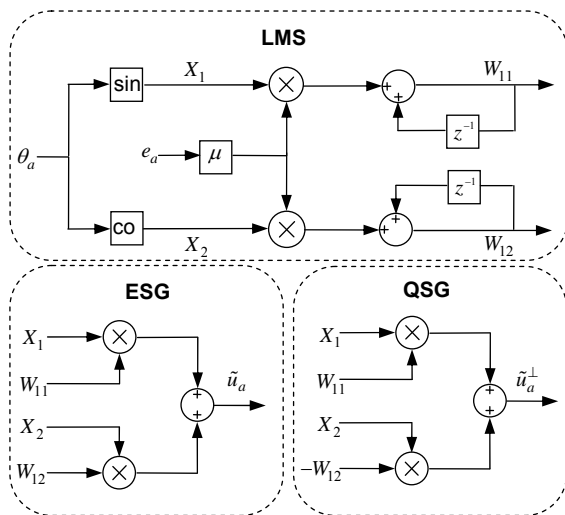


Fig. 1. Structure of LMS based adaptive filter

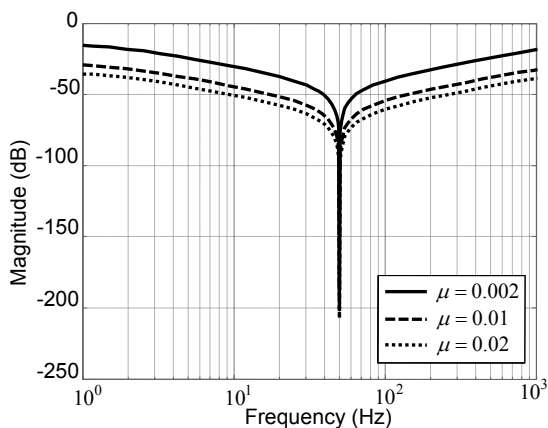


Fig. 2. Bode diagram of LMS based adaptive filter

2 Instantaneous Symmetrical Components Theory

Aforementioned strategy can easily be implemented to estimate three phase voltages. To extract grid sequence,

symmetrical components theory [30-32] is introduced as follows. The three phase set of estimated signals can be expressed as: $\tilde{Y} = \tilde{Y}^+ + \tilde{Y}^- + \tilde{Y}^0$, where, \tilde{Y}^+ , \tilde{Y}^- and \tilde{Y}^0 are positive, negative, and zero sequence components. Considering that some of the three phase grid connected power converters employ a four wire connection, it is necessary to be synchronized with zero sequence of the grid voltage. The instantaneous symmetrical components are related to the input signal by the equations:

$$\begin{aligned}
\tilde{Y}^+ &= \begin{bmatrix} \tilde{u}_a^+ \\ \tilde{u}_b^+ \\ \tilde{u}_c^+ \end{bmatrix} = \frac{1}{3} \begin{bmatrix} 1 & \beta & \beta^2 \\ \beta^2 & 1 & \beta \\ \beta & \beta^2 & 1 \end{bmatrix} \begin{bmatrix} \tilde{u}_a \\ \tilde{u}_b \\ \tilde{u}_c \end{bmatrix} = T^+ \tilde{Y} \\
\tilde{Y}^- &= \begin{bmatrix} \tilde{u}_a^- \\ \tilde{u}_b^- \\ \tilde{u}_c^- \end{bmatrix} = \frac{1}{3} \begin{bmatrix} 1 & \beta^2 & \beta \\ \beta & 1 & \beta^2 \\ \beta^2 & \beta & 1 \end{bmatrix} \begin{bmatrix} \tilde{u}_a \\ \tilde{u}_b \\ \tilde{u}_c \end{bmatrix} = T^- \tilde{Y} \\
\tilde{Y}^0 &= \begin{bmatrix} \tilde{u}_a^0 \\ \tilde{u}_b^0 \\ \tilde{u}_c^0 \end{bmatrix} = \frac{1}{3} \begin{bmatrix} 1 & 1 & 1 \\ 1 & 1 & 1 \\ 1 & 1 & 1 \end{bmatrix} \begin{bmatrix} \tilde{u}_a \\ \tilde{u}_b \\ \tilde{u}_c \end{bmatrix} = T^0 \tilde{Y}
\end{aligned}
\quad (18)$$

where $\beta = -\frac{1}{2} + \frac{\sqrt{3}}{2}j$. j stands for a 90 degrees phase shift operator in the time domain. β can be split into its real part and imaginary part, then equation (18) can be rewritten as:

$$(19) \quad \begin{cases} \tilde{Y}^+ = T_1 \tilde{Y} + T_2 \tilde{Y}^\perp \\ \tilde{Y}^- = T_1 \tilde{Y} - T_2 \tilde{Y}^\perp \\ \tilde{Y}^0 = T_3 \tilde{Y} \end{cases}$$

where T_1 , T_2 and T_3 are 3×3 matrices given by:

$$\begin{aligned}
(20) \quad T_1 &= \frac{1}{3} \begin{bmatrix} 1 & -0.5 & -0.5 \\ -0.5 & 1 & -0.5 \\ -0.5 & -0.5 & 1 \end{bmatrix} \\
T_2 &= \frac{1}{2\sqrt{3}} \begin{bmatrix} 0 & 1 & -1 \\ -1 & 0 & 1 \\ 1 & -1 & 0 \end{bmatrix} \\
T_3 &= \frac{1}{3} \begin{bmatrix} 1 & 1 & 1 \\ 1 & 1 & 1 \\ 1 & 1 & 1 \end{bmatrix}
\end{aligned}$$

As shown in equation (19), if the estimated signal \tilde{Y} and its orthogonal version \tilde{Y}^\perp are known, then the linear matrix transformation can be used to extract the grid sequence components. Since the LMS behaves as an in-quadrature signals generator itself, the positive, negative, and zero sequence components of the three phase signals can be obtained by means of using a LMS for each phase voltage.

3 Phase Locked Loop

From the abovementioned analysis, it is clear that the proposed strategy can achieve the accurate symmetrical components extraction on condition that θ_a is estimated accurately. In practice, grid voltage may experience phase angle jump or frequency variation. To ensure that the proposed grid sequence detector gives rise to precise

results it is necessary to equip the system with phase locked ability. The basic configuration of the phase angle estimation is shown in Fig. 3.

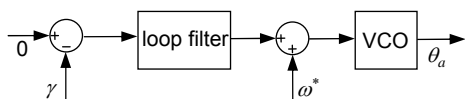


Fig. 3. Block diagram of the PLL system

The feedback component γ can be expressed as:

$$\begin{aligned} \gamma &= \frac{W_{12}}{\sqrt{W_{11}^2 + W_{12}^2}} \\ (21) \quad &= \frac{U_a^1 \sin(\varphi_a)}{\sqrt{(U_a^1)^2 \cos^2(\varphi_a) + (U_a^1)^2 \sin^2(\varphi_a)}} \\ &= \sin(\varphi_a) \end{aligned}$$

It can be noticed that γ contains information of estimated phase error that is then utilized as the input for the loop filter. The discrete proportional-integral (PI) type controller is chosen to obtain a good trade-off between the filter performance and system stability. If it is assumed that φ_a is very small, the term $\sin(\varphi_a)$ behaves linearly, i.e., $\sin(\varphi_a) \approx \varphi_a$ [1]. Therefore, the PLL can be treated as a linearized model. The block diagram of the PLL system in the discrete time domain is shown in Fig. 4. The block $K_d(z)$ is the z transform of the loop filter and voltage controlled oscillator (VCO). The closed loop transfer function can be represented as [19]:

$$(22) \quad H_c(z) = \frac{K_d(z)}{1 + K_d(z)}$$

For the second order loop using the PI type filter, $K_d(z)$ can be obtained as:

$$(23) \quad K_d(z) = k_p \frac{z(z-\alpha)}{(z-1)^2}$$

where $\alpha = 1 - T_s/\tau$. T_s denotes the sampling period of the digital system. k_p and τ denote the gains of the PI type loop filter. Fig. 5 shows the root loci of the closed loop system. It can be observed that there are two open loop poles at $z=1$ and two open loop zeros at $z=0$ and $z=\alpha$. When $T_s > 2\tau$, the closed loop system is unstable in which the open loop zero α is located at the outside of unit circle.

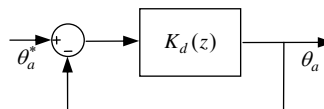


Fig. 4. Simplified z domain model of PLL

4 Description of the Main Structure

The main structure of the proposed LMS-PLL synchronization method for grid sequence extraction is presented in Fig. 6, which consists of least mean square (LMS-a, LMS-b, LMS-c) blocks, phase locked loop (PLL) block, and symmetrical components calculator (SCC) block. The detailed implementation block diagram of parallel units (LMS-a, LMS-b, LMS-c) and phase locked loop (PLL) are shown in Fig. 1 and Fig. 3. It can be noticed that the PLL output θ_a is treated as input data for LMS filters and the weight coefficient γ is treated as the only feedback component for PLL block. The estimated each phase input

signal and its 90 degrees phase shift version are forwarded to a computational unit (SCC) which calculates the symmetrical components using a linear transformation. In SRF-PLL, the occurrence of any phase voltage fault will cause a large deviation of phase angle estimation. By contrast, in the presented algorithm, other two faulty signals have no impact on phase angle estimation because the PLL block is only connected to the LMS-a for synchronization.

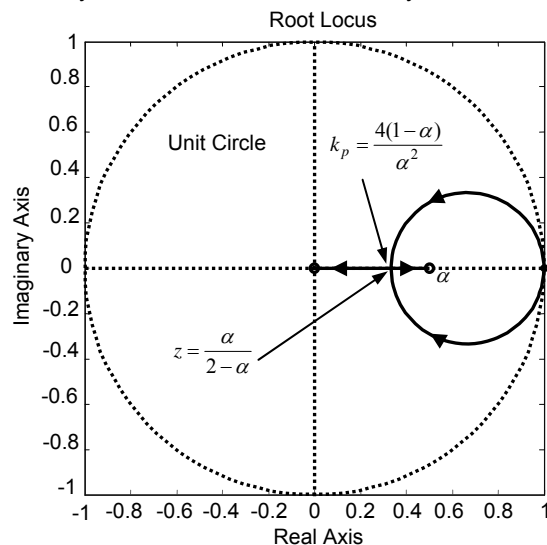


Fig. 5. Root locus of simplified PLL in z domain

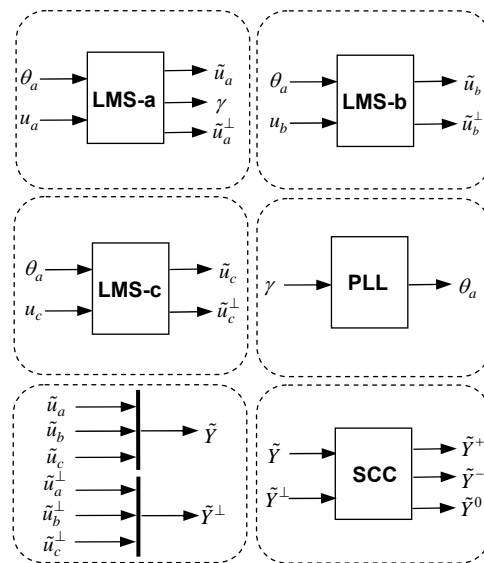


Fig. 6. Scheme of the proposed LMS-PLL

5 Multiple LMS Adaptive Filter

Thanks to LMS inherent filtering characteristic, it is able to perform an accurate estimation of the fundamental component of the input voltage under unbalanced and small distorted conditions. However, the extraction error will not be acceptable when the low order harmonics is relatively large. To make the proposed system faster while rejecting harmonics, in this section, a new structure named as the multiple LMS (MLMS) is proposed to accurately detect the specified harmonic sequences of the grid voltage, even under extreme distorted conditions. Fig. 7 shows the MLMS structure, as it can be noticed, the MLMS can be understood as a set of n selective and adaptive filters, tuned at different frequencies and working in parallel. The LMS-n block has the similar structure with Fig. 1 except that

the input θ_a (in Fig. 1) is replaced by $n\theta_a$ (in Fig. 7), the estimated error $e_a = u_a - \tilde{u}_a$ (in Fig. 1) is replaced by

$$e_a = u_a - \sum_{x=1}^n \tilde{u}_{xa} \quad (\text{in Fig. 7}).$$

It can be observed that the number of separated harmonics depends directly on the number of subfilters. If the proposed MLMS structure is extended to three phase systems, a fast and precise extraction of the fundamental and other harmonic grid sequence components is guaranteed. Similar to equation (17), the transfer function from estimated error e_a to the LMS-n block output \tilde{u}_{na} in Fig. 7 is given by:

$$G_n(z) = \frac{\mu(1 - z^{-1} \cos n\omega T_s)}{T_s(1 - 2z^{-1} \cos n\omega T_s + z^{-2})} \quad (24)$$

For the special case, only the fundamental, 5th and 7th components are considered. Therefore, the generalized transfer function from instantaneous estimated error to estimated each phase voltage can be expressed as:

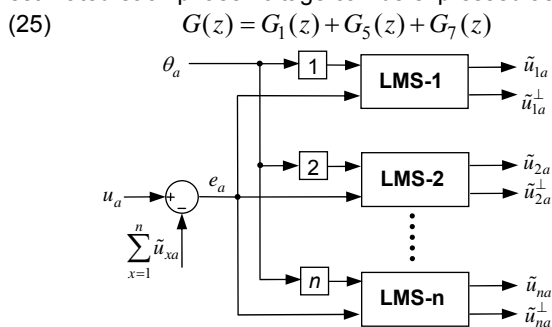


Fig. 7. Block diagram of MLMS filter structure

The dashed line in Fig. 8 shows the discrete bode diagram of the transfer function given by equation (25). It can be observed in this diagram how the multiple structure gives rise to notches in the frequency response curve at the frequencies where the individual LMS-n is tuned. As a result, this configuration guarantees better performance in case of high distorted level.

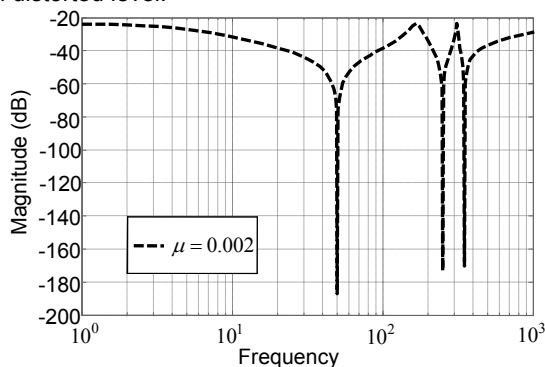


Fig. 8. Bode diagram of the MLMS where fundamental, 5th and 7th harmonic components are included

Simulation Results

In order to evaluate performance of the proposed algorithm, the time domain simulations are carried out by means of MATLAB/SIMULINK, using the fixed step discrete time solver at $f_s = 5kHz$. Initial parameters have been selected as follows: The step size of the adaptive filter is set to $\mu = 0.06$, The parameters of the PLL are set to $k_p = 2.63$ and $\tau = 0.034$. The initial three phase grid voltage is balanced and undistorted. Its amplitude and

fundamental frequency are 1 p.u. and 50Hz respectively. The following test cases have been considered for the utility voltage.

Case 1: Unbalance and Frequency Variation

The immunity of the proposed structure with respect to amplitude variation and the unbalanced condition is tested here, which is a common practice in distribution systems or grid connected converters. In this case, the fundamental positive sequence is reduced to 0.6 p.u.. Meanwhile, 0.3 p.u. negative sequence and 0.1 p.u. zero sequence are added to the initial voltage at 1.1s. Moreover, to set a more serious circumstance, when $t = 1s$, the frequency starts increasing at 15 Hz/s and it reaches 53 Hz at 1.2s.

Fig. 9 shows the transient response of the LMS-PLL under the aforementioned condition. It can be observed that the proposed method can accurately extract the positive, negative and zero sequences with almost imperceptible transient time. The frequency tracking capabilities of the proposed and other methods are shown in Fig. 10. Notice that, all methods provide a fast and accurate response during normal conditions. However, under unbalanced situation, The SRF-PLL can not lock the phase angle well. The DDSRF-PLL and DSOGI-PLL have higher transitory error, but fast response, while the 3ph-ELL has slower dynamics. Only the proposed technique has a good compromise between dynamic response and steady precision.

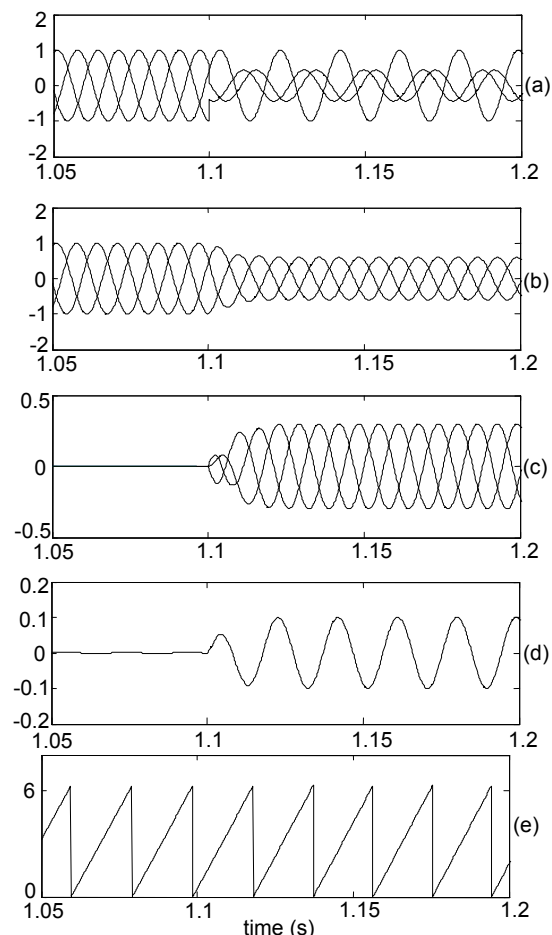


Fig.9. LMS-PLL simulation results when grid voltage is suffering from unbalance and frequency variation. (a) grid voltage [p.u.]. (b) 1st positive sequence [p.u.]. (c) 1st negative sequence [p.u.]. (d) 1st zero sequence [p.u.]. (e) detected phase angle [rad].

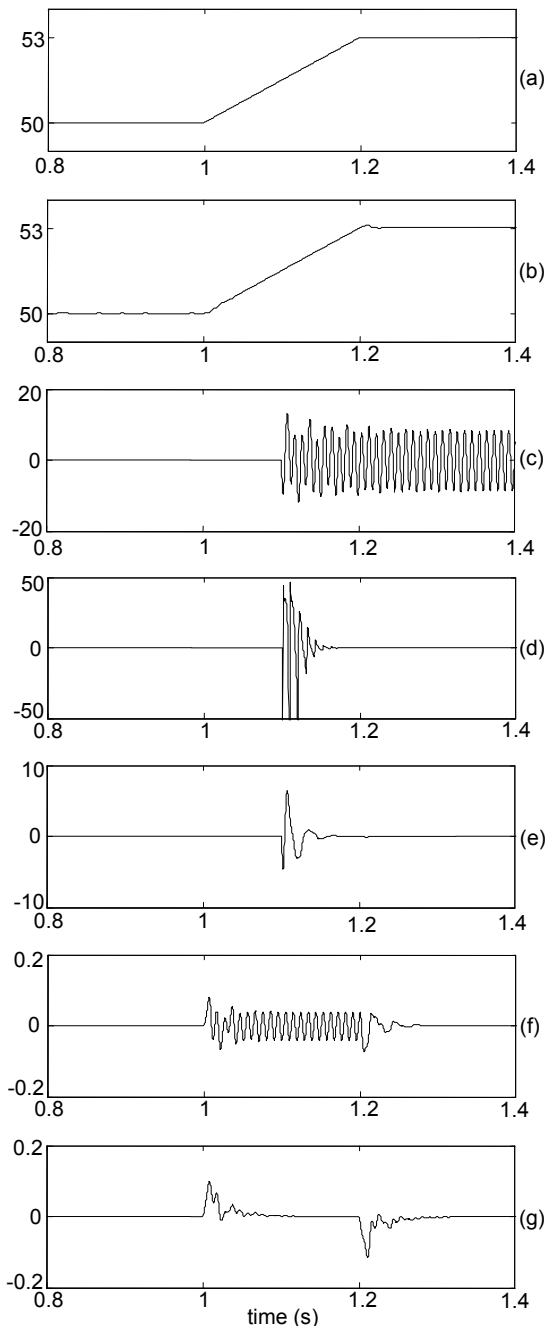


Fig. 10. Grid frequency estimation performance of PLLs in case 1. (a) real value of grid frequency [Hz]. (b) detected frequency with LMS-PLL [Hz]. (c) estimated error with SRF-PLL [Hz]. (d) estimated error with DDSRF-PLL [Hz]. (e) estimated error with DSOGI-PLL [Hz]. (f) estimated error with 3ph-EPLL [Hz]. (g) estimated error with LMS-PLL [Hz].

Case 2: Unbalance and Harmonics

In this case, unbalanced and highly distorted three phase grid voltages are considered for simulation tests. Similar to Case 1, the fundamental negative and zero sequence components are superposed on the 0.6 p.u. positive sequence with the values of 0.3 p.u. and 0.1 p.u. during the fault. Furthermore, the harmonic components set is added as follows: fifth (0.1 p.u. negative sequence), seventh (0.06 p.u. positive sequence).

As it can be appreciated in Fig. 11(d), the LMS-PLL structure can't achieve the accurate extraction for sequence components when the input voltage is highly polluted. In contrast, due to the selective harmonic separating characteristic, MLMS-PLL can overcome the weakness

mentioned. As shown in Fig. 11(b), (c), (e)–(g), this configuration is able to acquire the accurate estimation of the fundamental and harmonic grid sequences.

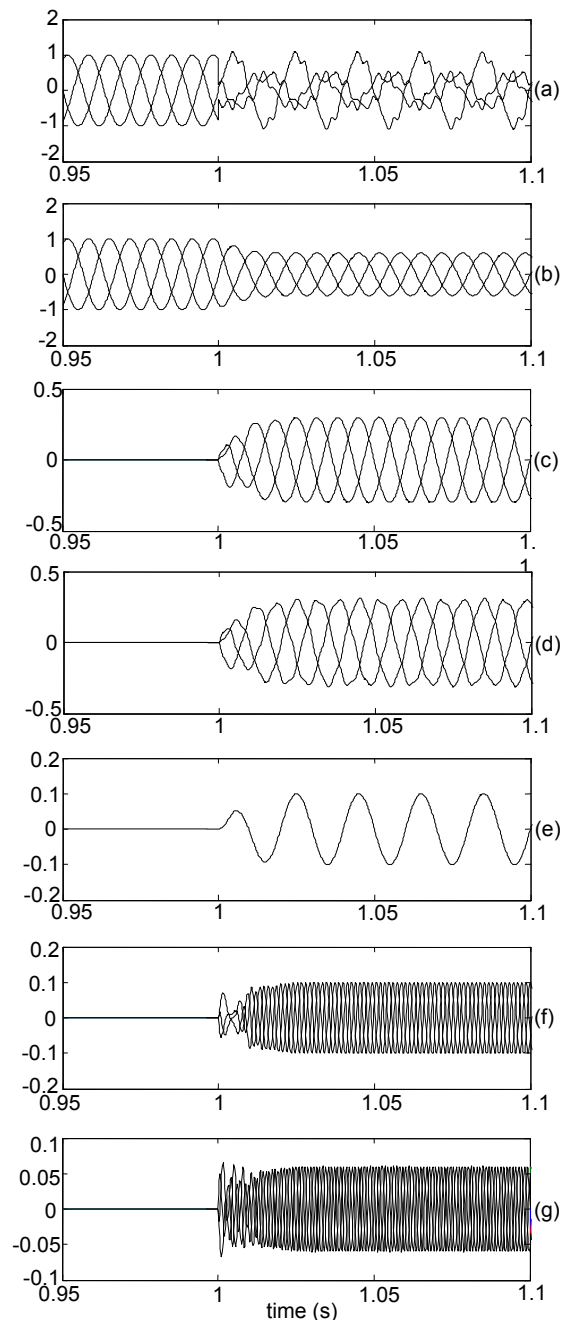


Fig. 11. MLMS-PLL simulation results when grid voltage is suffering from unbalance and harmonics. (a) grid voltage [p.u.]. (b) 1st positive sequence [p.u.]. (c) 1st negative sequence [p.u.]. (d) 1st negative sequence with LMS-PLL [p.u.]. (e) 1st zero sequence [p.u.]. (f) 5th negative sequence [p.u.]. (g) 7th positive sequence [p.u.].

Fig. 12 shows some plots regarding frequency estimated error detected by the representative PLL algorithms. It can be observed that LMS based PLLs have the minimum oscillating ripple. Especially, the MLMS-PLL completely corrects the error after a short transient time.

Experimental Results

To verify the effectiveness of the proposed synchronization algorithm in this paper, the system was implemented in a control board based on the dSPACE 1005 experimental platform. All the required signals are

programmed by the Chroma 61512 AC source, which can generate voltage dip or rise, phase angle jump, harmonics, unbalance, frequency offset and other typical fault signals. The input signals have been acquired through the DS2003 A/D board, and processed in dSPACE 1005. Control Desk is used to display the variables on the computer screen. Fig. 13 shows a basic diagram of the experimental setup.

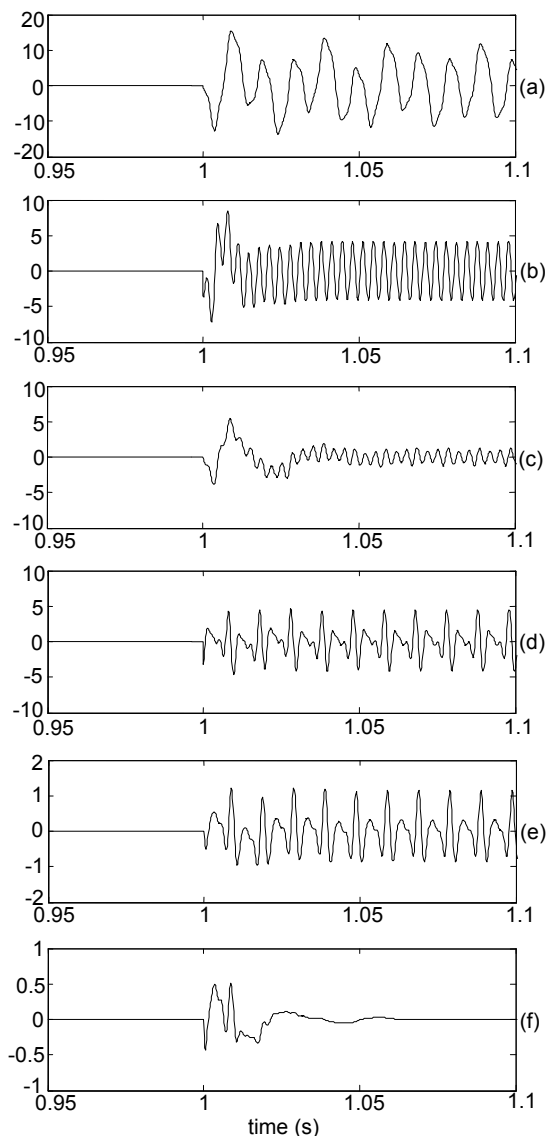


Fig. 12. Grid frequency estimated error of PLLs in case 2. (a) estimated error with SRF-PLL [Hz]. (b) estimated error with DDSRF-PLL [Hz]. (c) estimated error with DSOGI-PLL [Hz]. (d) estimated error with 3ph-EPLL [Hz]. (e) estimated error with LMS-PLL [Hz]. (f) estimated error with MLMS-PLL [Hz].

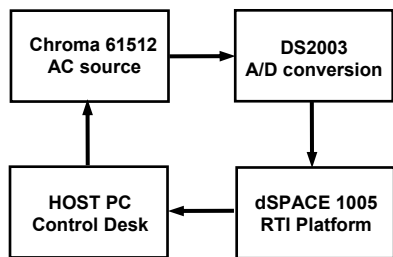


Fig. 13. Block diagram of experimental setup

Experimental situation and parameters selection is the same as case 2, presented in simulation. Fig. 14 shows the experimental results. Fig. 14(a)–(c) show that the fast

response and accurate performance of the proposed MLMS-PLL are revealed even when the measured signal is simultaneously affected by harmonics and unbalance. As shown in Fig. 14(d), the fundamental negative symmetrical components detected by MLMS-PLL entirely eliminate harmonics influence and reach the correct value after a relatively short transient. However, due to lack of multiple structure, LMS-PLL shows obvious oscillation in the estimated fundamental negative sequence.

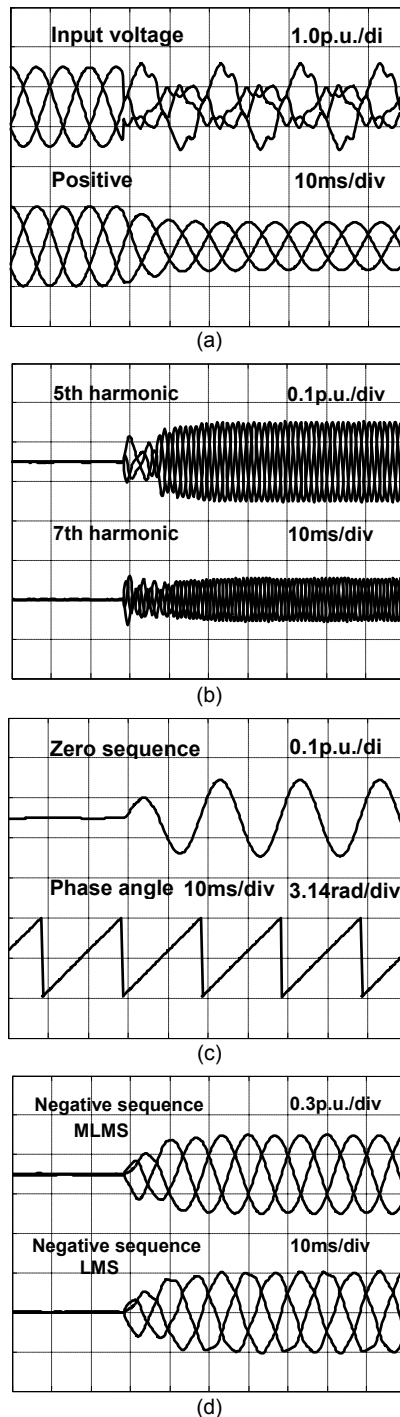


Fig.14. Experimental results when grid voltage is suffering from unbalance and harmonics. (a) input voltage and detected 1st positive sequence with MLMS-PLL. (b) detected 5th negative and 7th positive sequences with MLMS-PLL. (c) detected 1st zero sequence and phase angle with MLMS-PLL. (d) detected 1st negative sequence with LMS-PLL and MLMS-PLL.

Comparison

To highlight the features of the proposed method, in this section, the performance assessment of several PLL algorithms is carried out. As shown in Table I, it is noticed that SRF-PLL has the shortest settling time with the lowest computational burden but the phase tracking performance is limited under unbalanced or distorted grid conditions. DDSRF-PLL and DSOGI-PLL have similar performance on phase tracking and computational burden, while the former has shorter response time. 3ph-EPLL and LMS-PLL have better antiharmonic characteristic than aforementioned methods, although they have relatively high computational burden. The last column in Table I summarizes the performance of MLMS-PLL method. It can be observed that

MLMS-PLL has shorter settling time and zero phase estimated error at the cost of computational burden. It must be pointed out that with the development of digital signal processors, computational burden is no longer a problem. In addition, the last three algorithms have special structures with no need of coordinate transformation. The application field of PLL methods is described in Table II, it can be observed that only the proposed MLMS-PLL can realize accurate phase locked control when there are harmonics and unbalance in grid voltage. From Table III, it is noticed that only the proposed MLMS-PLL can extract the fundamental and harmonic symmetrical components of three phase input signals.

Table I. Performance comparison of PLL methods

	SRF-PLL	DDSRF-PLL	DSOGI-PLL	3ph-EPLL	LMS-PLL	MLMS-PLL
Settling time	< 40ms	≈ 40ms	> 40ms	> 40ms	≈ 40ms	≈ 40ms
Phase error (unbalanced)	≠ 0	= 0	= 0	= 0	= 0	= 0
Phase error (distorted)	≠ 0	≠ 0	≠ 0	≠ 0	≠ 0	= 0
Computational burden	lowest	low	low	high	high	highest
Clarke transformation	need	need	need	no need	no need	no need
Park transformation	need	need	need	no need	no need	no need

Table II. Application field of PLL methods

		SRF-PLL	DDSRF-PLL	DSOGI-PLL	3ph-EPLL	LMS-PLL	MLMS-PLL
Balanced	Undistorted	Y	Y	Y	Y	Y	Y
	Distorted lightly	Y	Y	Y	Y	Y	Y
	Distorted heavily	N	N	N	N	N	Y
Unbalance d	Undistorted	Y	Y	Y	Y	Y	Y
	Distorted lightly	Y	Y	Y	Y	Y	Y
Unbalance d lightly	Distorted heavily	N	N	N	N	N	Y
	Undistorted	N	Y	Y	Y	Y	Y
Unbalance d heavily	Distorted lightly	N	Y	Y	Y	Y	Y
	Distorted heavily	N	N	N	N	N	Y

Notes: Y -- well locked; N -- unlocked;

Table III. Separated grid sequence of PLL methods

		SRF-PLL	DDSRF-PLL	DSOGI-PLL	3ph-EPLL	LMS-PLL	MLMS-PLL
Fundamental	Positive	Y	Y	Y	Y	Y	Y
	Negative	N	Y	N	N	Y	Y
	Zero	N	N	N	N	Y	Y
Harmonic	Positive	N	N	N	N	N	Y
	Negative	N	N	N	N	N	Y
	Zero	N	N	N	N	N	Y

Conclusion

In this paper, a method based on LMS filter for obtaining grid sequence is presented and evaluated through theoretical analysis, simulation and experimental results which demonstrate the good performance of the strategy for distorted and unbalanced three phase systems. The main architecture consists of three parallel LMS or MLMS filters detecting each phase and its 90 degrees phase shift version which are delivered into a computational unit to calculate the symmetrical components using a linear transformation. Furthermore, a PLL based frequency adaptive scheme is also used for grid synchronization. Low computational burden due to recursive mode and no coordinate transformation makes the method suitable for software implementation, and the flexibility of the structure depends on harmonics to be considered for industrial applications.

Acknowledgement: This work was supported by the National Natural Science Foundation of China under Award 51107020.

REFERENCES

- [1] V. Kaura, V. Blasko, Operation of a phase locked loop system under distorted utility conditions, IEEE Trans. Ind. Appl., vol. 33 n. 1, February 1997, pp. 58 – 63.
- [2] F. Blaabjerg, R. Teodorescu, M. Liserre, et al, Overview of control and grid synchronization for distributed power generation systems, IEEE Trans. Ind. Electron., vol. 53 n. 5, October 2006, pp. 1398 – 1409.
- [3] D. Jovcic, Phase locked loop system for FACTS, IEEE Trans. Power Syst., vol. 18, no. 3, August 2003, pp. 1116 – 1124.
- [4] I. Etxeberria-Otadui, U. Viscarret, M. Caballero, et al, New optimized PWM VSC control structures and strategies under

- unbalanced voltage transients, *IEEE Trans. Ind. Electron.*, vol. 54 n. 5, October 2007, pp. 2902 – 2914.
- [5] Q. Song, W. Liu, Control of a cascade STATCOM with star configuration under unbalanced conditions, *IEEE Trans. Power Electron.*, vol. 24 n. 1, January 2009, pp. 45 – 58.
- [6] F. D. Freijedo, J. Doval-Gandoy, O. Lopez, et al, A signal-processing adaptive algorithm for selective current harmonic cancellation in active power filters, *IEEE Trans. Ind. Electron.*, vol. 56 n. 8, August 2009, pp. 2829 – 2840.
- [7] C. H. da Silva, R. R. Pereira, L. E. Borges da Silva, et al, A digital PLL scheme for three-phase system using modified synchronous reference frame, *IEEE Trans. Ind. Electron.*, vol. 56 n. 8, August 2009, pp. 3814 – 3821.
- [8] M. Dai, M. N. Marwali, J.-W. Jung, and A. Keyhani, Power flow control of a single distributed generation unit, *IEEE Trans. Power Electron.*, vol. 23 n. 1, January 2008, pp. 343 – 352.
- [9] C. H. Ng, L. Ran, and J. Bumby, Unbalanced-grid-fault ride-through control for a wind turbine inverter, *IEEE Trans. Ind. Appl.*, vol. 44 n. 3, May 2008, pp. 845 – 856.
- [10] S. Alepuz, S. Busquets-Monge, J. Bordonau, J. A. Martinez-Velasco, C. A. Silva, J. Pontt, and J. Rodriguez, Control strategies based on symmetrical components for grid-connected converters under voltage dips, *IEEE Trans. Ind. Electron.*, vol. 56 n. 6, June 2009, pp. 2162 – 2173.
- [11] A. M. Salamah, S. J. Finney and B. W. Williams, Three-phase phase-lock loop for distorted utilities, *IET Electr. Power Appl.*, vol. 1 n. 6, November 2007, pp. 937 – 945.
- [12] A. V. Timbus, M. Liserre, F. Blaabjerg, R. Teodorescu, P. Rodriguez, PLL algorithm for power generation systems robust to grid faults, the 37th IEEE Power Electronics Specialists Conference ~PESC' 2006~, June 18-22, 2006, Jeju, Korea.
- [13] R. M. S. Filho, P. F. Seixas, P. C. Cortizo, L. A. B. Torres, and A. F. Souza, Comparison of three single-phase pll algorithms for ups applications, *IEEE Trans. Ind. Electron.*, vol. 55 n. 8, August 2008, pp. 2923 – 2932.
- [14] P. Rodriguez, A. V. Timbus, R. Teodorescu, M. Liserre, and F. Blaabjerg, Flexible active power control of distributed power generation systems during grid faults, *IEEE Trans. Ind. Electron.*, vol. 54 n. 5, October 2007, pp. 2583 – 2592.
- [15] L. Asiminoaei, F. Blaabjerg, and S. Hansen, Detection is key – harmonic detection methods for active power filter applications, *IEEE Ind. Appl. Mag.*, vol. 13 n. 4, July/ August 2007, pp. 22 – 33.
- [16] O. Vainio and S. J. Ovaska, Digital filtering for robust 50/60 Hz zero crossing detectors, *IEEE Trans. Instrum. Meas.*, vol. 45 n. 2, April 1996, pp. 426 – 430.
- [17] O. Vainio and S. J. Ovaska, Noise reduction in zero crossing detection by predictive digital filtering, *IEEE Trans. Ind. Electron.*, vol. 42 n. 1, February 1995, pp. 58 – 62.
- [18] M. B. Duric and Z. R. Durisic, Frequency measurement in power networks in the presence of harmonics using fourier and zero crossing technique, *IEEE St. Petersburg Power Tech Conference ~SPPT' 2005~, June 27-30, 2005, St. Petersburg, Russia.*
- [19] S.-K. Chung, A phase tracking system for three phase utility interface inverters, *IEEE Trans. Power Electron.*, vol. 15 n. 3, May 2000, pp. 431 – 438.
- [20] L.G. Barbosa Rolim, D. Rodrigues da Costa Jr, and M. Aredes, Analysis and software implementation of a robust synchronizing PLL circuit based on the pq theory, *IEEE Trans. Ind. Electron.*, vol. 53 n. 6, December 2006, pp. 1919 – 1926.
- [21] P. Rodríguez, J. Pou, J. Bergas, I. Candela, R. Burgos, and D. Boroyevich, Decoupled double synchronous reference frame PLL for power converters control, *IEEE Trans. Power Electron.*, vol. 22 n. 2, March 2007, pp. 584 – 592.
- [22] M. Ciobotaru, R. Teodorescu, and F. Blaabjerg, A new single-phase PLL structure based on second order generalized integrator, the 37th IEEE Power Electronics Specialists Conference ~PESC' 2006~, June 18-22, 2006, Jeju, Korea.
- [23] P. Rodriguez, A. Luna, M. Ciobotaru, R. Teodorescu, and F. Blaabjerg, Advanced grid synchronization system for power converters under unbalanced and distorted operating conditions, the 32nd IEEE Annual Conference on Industrial Electronics ~ IECON 2006~, November 7-10, 2006, Paris, France.
- [24] P. Rodriguez, R. Teodorescu, I. Candela, A. Timbus, M. Liserre, and F. Blaabjerg, New positive-sequence voltage detector for grid synchronization of power converters under faulty grid conditions, the 37th IEEE Power Electronics Specialists Conference ~PESC' 2006~, June 18-22, 2006, Jeju, Korea.
- [25] M. K. Ghartemani and M. R. Iravani, A nonlinear adaptive filter for online signal analysis in power systems applications, *IEEE Trans. Power Del.*, vol. 17 n. 2, April 2002, pp. 617 – 622.
- [26] M. Karimi-Ghartemani, M. R. Iravani, A method for synchronization of power electronic converters in polluted and variable-frequency environments, *IEEE Trans. Power Syst.*, vol. 19, no. 3, August 2004, pp. 1263 – 1270.
- [27] A. K. Pradhan, A. Toutray, and A. Basak, Power system frequency estimation using least mean square technique, *IEEE Trans. Power Del.*, vol. 20 n. 3, July 2005, pp. 1812 – 1816.
- [28] Q. Ai, Y. Zhou, and W. Xu, Adaline and its application in power quality disturbances detection and frequency tracking, *Electric Power Systems Research*, vol. 77 n. 5-6, April 2007, pp. 462 – 469.
- [29] Wang, Z.-Q., Manry, M. T., and Schiano, J. L., LMS learning algorithm: Misconceptions and new results on convergence, *IEEE Trans. Neural Netw.*, vol. 11 n. 1, January 2000, pp. 47 – 56.
- [30] C. L. Fortescue, Method of symmetrical coordinates applied to the solution of polyphase networks, *Trans. AIEE*, vol. 37 n. 2, 1918, pp. 1027 – 1140.
- [31] W. V. Lyon, Application of the Method of Symmetrical Components (McGraw-Hill, Inc., 1937).
- [32] G. C. Paap, Symmetrical components in the time domain and their application to power network calculations, *IEEE Trans. Power Syst.*, vol. 15, n. 2, May 2000, pp. 522 – 528.

Authors: lecturer. Xueguang Zhang, Department of Electrical Engineering, Harbin Institute of Technology, Harbin 150001, E-mail: xqhit@126.com; m.e.e. Dakun Duan, Department of Electrical Engineering, Harbin Institute of Technology, E-mail: dshhit2008@163.com; m.e.e. Jiaming Chen, Department of Electrical Engineering, Harbin Institute of Technology, E-mail: jiaminghit@126.com; dr. Yicheng Liu, Department of Electrical Engineering, Harbin Institute of Technology, E-mail: liuyicheng19850828@163.com; prof. dr. Dianguo Xu, Department of Electrical Engineering, Harbin Institute of Technology, E-mail: xudiang@hit.edu.cn.

Corresponding Author: Xueguang Zhang, Department of Electrical Engineering, Harbin Institute of Technology, Harbin 150001, China. email: xqhit@126.com